

Versatile, Low-Cost, and Portable 2D Material Transfer Setup with a Facile and Highly Efficient DIY Inert-Atmosphere Glove Compartment Option

Kanokwan Buapan, Ratchanok Somphonsane, Tinna Chiawchan, and Harihara Ramamoorthy*

Cite This: *ACS Omega* 2021, 6, 17952–17964

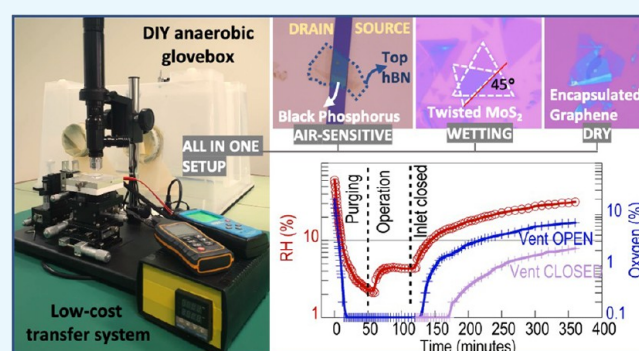
Read Online

ACCESS |

Metrics & More

Article Recommendations

ABSTRACT: Research in van der Waals heterostructures has been rapidly progressing in the past decade, thanks to the art of sequential and deterministic placement of one two-dimensional (2D) material over another. The successful creation of heterostructures however has relied largely on expensive transfer systems that are not easily accessible to researchers. Although a few reports on low-cost systems have recently surfaced, the full functionality, portability features, and overall effectiveness of such systems are still being explored. In this work, we present an “all-in-one” low-cost transfer setup that is compact, lightweight, and portable and which can be quickly installed with a facile and do it yourself (DIY)-style anaerobic glovebox option that performs at par with commercial anaerobic systems. The “installable” glovebox option means the user has the convenience of quickly converting the working environment into an inert one when air-sensitive 2D materials are used. The lowest RH values obtained in our glovebox is <3%, and the O₂ levels rapidly drop from 21% to less than 0.1% in just a few minutes of purging the chamber with inert gas. The transfer system is also equipped with a light-weight PID-controlled substrate heating option that can be easily assembled within just a few hours. We test the versatility of our low-cost system by the successful creation of hexagonal boron nitride (hBN)-encapsulated graphene and hBN-encapsulated molybdenum disulphide (MoS₂) heterostructures using the hot pickup technique and graphene-hBN, MoS₂-hBN, twisted MoS₂, and twisted MoS₂ on hBN stacks using the wetting technique, and a MoS₂-hBN-graphene vertical tunneling heterostructure was formed using a combination approach. The effectiveness of the DIY glovebox is proven with the demonstration of extended stability of freshly exfoliated black phosphorous (BP) flakes, their encapsulation between thin hBN layers, and the formation of electrically contacted BP devices with a protective hBN top layer. At an overall price point of approximately 1000 \$, the versatile setup presented here is expected to further contribute to the growth of research in 2D materials, in particular, for researchers initially faced with overcoming a huge entry-level threshold to work in the field of 2D materials and van der Waals heterostructures.



The lowest RH values obtained in our glovebox is <3%, and the O₂ levels rapidly drop from 21% to less than 0.1% in just a few minutes of purging the chamber with inert gas. The transfer system is also equipped with a light-weight PID-controlled substrate heating option that can be easily assembled within just a few hours. We test the versatility of our low-cost system by the successful creation of hexagonal boron nitride (hBN)-encapsulated graphene and hBN-encapsulated molybdenum disulphide (MoS₂) heterostructures using the hot pickup technique and graphene-hBN, MoS₂-hBN, twisted MoS₂, and twisted MoS₂ on hBN stacks using the wetting technique, and a MoS₂-hBN-graphene vertical tunneling heterostructure was formed using a combination approach. The effectiveness of the DIY glovebox is proven with the demonstration of extended stability of freshly exfoliated black phosphorous (BP) flakes, their encapsulation between thin hBN layers, and the formation of electrically contacted BP devices with a protective hBN top layer. At an overall price point of approximately 1000 \$, the versatile setup presented here is expected to further contribute to the growth of research in 2D materials, in particular, for researchers initially faced with overcoming a huge entry-level threshold to work in the field of 2D materials and van der Waals heterostructures.

1. INTRODUCTION

Research in van der Waals heterostructures has seen a sharp increase in recent years.^{1–6} This rapid progress is made possible, thanks to the art of deterministic placement of similar or dissimilar two-dimensional (2D) materials atop one another, leading to a plethora of possible combinations for creating stacked heterostructures with novel functionalities. Of significant interest lately are also stacked heterostructures containing a twist angle between the individually stacked 2D layers.^{7–9} Recent investigations of such architectures have led to some of the most important scientific breakthroughs of recent times. This apparent paradigm shift, which departs significantly from the study of conventional 3D materials, gives researchers the opportunity to explore the intriguing physics of novel structures and evaluate their potential applications for the future.

In general, while research in 2D materials has rapidly accelerated over the past decade, it has not yet gained enough traction in several developing economies around the world. Part of the reason for this disparity is the lack of availability of research funds and/or state-of-the-art equipment needed to successfully carry out investigative tasks. For many researchers, working in the area of 2D materials is therefore seen as challenging and hard to execute.

Received: March 24, 2021

Accepted: June 25, 2021

Published: July 7, 2021

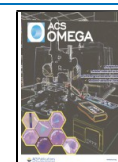


Table 1. List of All Parts Required, with Sourcing Details and Associated Costs, for Building the Low-Cost System

| category | function/provision | description | source | model/part# | price (\$) | |
|-----------------------------|---|--|--|--------------------------|-------------------|-----|
| (1) base unit ~1050 \$ | imaging system (~\$ 370) | 1000× inspection zoom monocular C-mount lens + coaxial light + stereo stand | www.aliexpress.com | | 226 | |
| | | auxiliary 5× objective lens | www.aliexpress.com | | 50 | |
| | | 5MP CMOS USB microscope camera | www.aliexpress.com | | 35 | |
| | stages (~\$ 390) | auxiliary camera | monitor | www.lazada.co.th | | 10 |
| | | | | www.lazada.co.th | | 52 |
| | | XYZR linear stage | | www.aliexpress.com | | 267 |
| | | | | www.aliexpress.com | | 127 |
| | substrate heating (~\$ 70) | configurable aluminum/A6061P plate | | https://th.misumi-ec.com | A6061FNN-80-80-12 | 24 |
| | | | fluororesin plates (80 × 80 × 10 mm) | https://th.misumi-ec.com | PTFE-80-80-10 | 15 |
| | | 0–1300 degree digital PID kit | www.aliexpress.com | | 15 | |
| | | 6 × 60 mm, 90 W, 220 V cartridge heater | www.aliexpress.com | | 6 | |
| | | electronic enclosure box | th.rs-online.com | 192-0756 | 8 | |
| | | high-temperature (up to 120°) double-sided PCB heat sink tape for securing the substrate | www.aliexpress.com | | 1.6 | |
| | | vibration isolation (~\$ 43) | vibration damping rubber feet (set of 8) | https://th.misumi-ec.com | KK-3012-30 | 18 |
| | | | vibration damping rubber mat | https://th.misumi-ec.com | EA997XC-1 | 9 |
| | | DIY glovebox setup (~\$ 170) | general purpose cutting mat (A1 size) | www.lazada.co.th | | 16 |
| | | | enclosure (storage box) | www.ikea.com | SAMLA 130 L | 16 |
| | portable humidity meter | | www.aliexpress.com | SNDWAY SW572 | 23 | |
| | portable oxygen meter | | www.aliexpress.com | AS8901 | 86 | |
| | large hose clamps (for securing gloves) | | www.aliexpress.com | | 3.5 | |
| | laboratory-resistant anaerobic gloves (1 set) | | www.aliexpress.com | | 15 | |
| | EPDM foam seal (4 m) | | https://th.misumi-ec.com | 686 × 10 × 15 | 9 | |
| | (2) optional upgrades | compact ball valves (for inert gas inlet and outlet) | | https://th.misumi-ec.com | BBPH61-B | 22 |
| | | | Standa www.standa.lt | 1BS-2040-015 | 160 | |
| system base | | optical breadboard | | | | |
| imaging system | | metallurgical microscope | Ningbo Sunny Instruments | MXFMS | 2000 | |
| substrate vacuum | | oil-free vacuum pump | www.rocker.com.tw | Rocker 300 | 230 | |
| | miniature vacuum hose fitting | https://th.misumi-ec.com | LHN-0640-M5 | 3 | | |
| (3) consumables ~1200 \$ | 2D materials (bulk) | KISH graphite (1 g) | https://graphene-supermarket.com | SKU-NKG-50-100 | 150 | |
| | | hBN flakes | NIMS Japan | BLK-Flks-BPs | gratis | |
| | | black phosphorus crystals | https://www.2dsemiconductors.com | | 430 | |
| | CVD precursors for MoS ₂ growth | molybdenum dioxide powder (10 g) | Merck www.sigmaaldrich.com | 234761-10G | 50 | |
| | | sulfur powder (10 g) | Merck www.sigmaaldrich.com | 213292-10G | 59 | |
| | substrate | 4 in. Si/300 nm SiO ₂ wafers | BIOTAIN www.crystal-material.com | | 36 | |
| | | prefabricated Pt test chips | https://www.ossila.com/ | S403A1 | 112 | |
| | exfoliation | 3M magic tape | www.officemate.co.th | OFM3000159 | 1.8 | |
| | PDMS/PPC stamp creation | Dow Corning sylgard 184: base and curing agent | www.ebay.com | | 126 | |
| | | PPC | Merck www.sigmaaldrich.com | 389021-25G | 131 | |
| anisole | | Merck www.sigmaaldrich.com | 123226-100ML | 107 | | |

Typically, the experimental setups used for the deterministic transfer and subsequent stacking of 2D materials are very expensive. The high cost is generally associated with the use of precision optics and mechanical components to achieve a high level of vibration isolation. Today, such systems are available

commercially as well. For instance, www.hqgraphene.com provides a transfer setup that costs approximately 21,000 \$. Many conventional transfer systems are based on retrofitting already existing mask aligners,¹⁰ metallurgical microscopes, and probe stations.¹¹ While this option may appear to be cost-

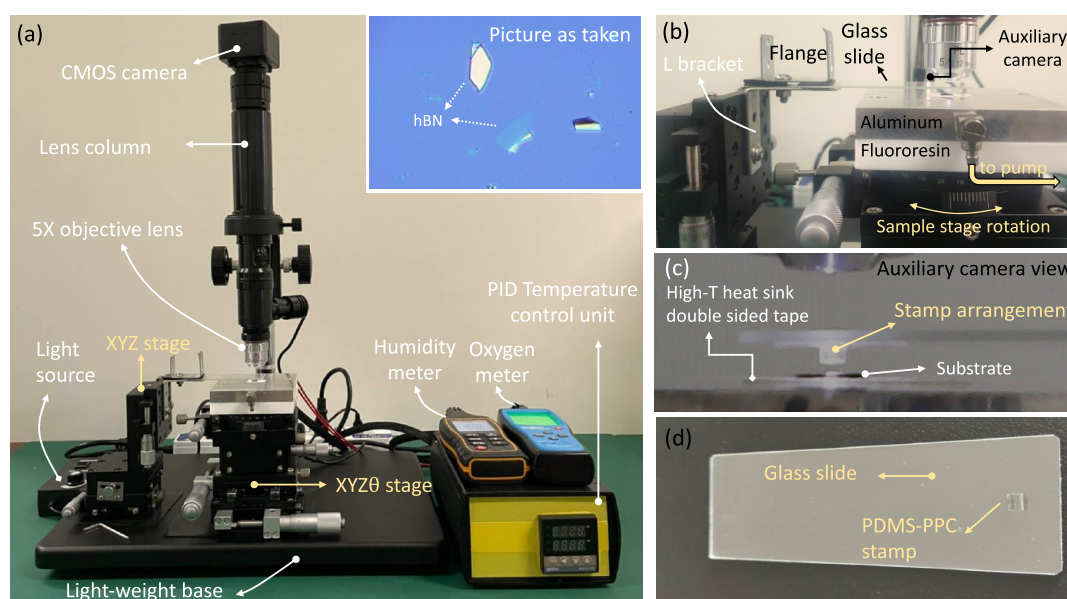


Figure 1. (a) Picture showing the main components of the low-cost 2D material transfer system. The inset shows the optical image taken at the maximum zoom level of the imaging system. (b) Zoomed-in picture showing how the glass slide and stamp assembly is affixed to the XYZ stage. Also seen here are the options for sample vacuum, auxiliary camera, and sample stage rotation. (c) Lateral view obtained from the auxiliary camera showing the relative position of the stamp and substrate. (d) Picture of the PDMS-PPC stamp affixed onto a glass slide. "All photographs courtesy of "Ratchanok Somphonsane". Copyright 2021."

effective for research groups already having access to these equipments, it is a nonstarter for young researchers working in small- to medium-sized laboratory settings where there is no access to such sophisticated systems. Moreover, these transfer systems end up being bulky and immobile and having a large footprint, making its practicality questionable.

These existing challenges make clear that there is an urgent need for other alternatives. While there is much to do in this regard, the first step in the right direction is to make budget-friendly and custom-designable 2D material transfer systems readily available to research groups across the globe. Very recently, such low-cost systems have been demonstrated^{12–14} and their effectiveness was proven with the successful assembly of high-quality heterostructures. In ref 12, a low-cost setup under 1100 \$ was used to transfer a thin InSe flake onto prepatterned gold electrodes. The researchers were also able to transfer a hexagonal boron nitride (hBN)-encapsulated InSe flake using the same setup. In ref 13, a similar low-cost system, albeit with slightly increased functionality, was employed to create hBN-WSe₂-hBN heterostructures. Here, the use of a heated sample stage allowed for employing the hot pickup process. In ref 14, the researchers have gone a step further and demonstrated the creation of hBN-encapsulated black phosphorous (BP) heterostructures in an inert-atmosphere gloveless anaerobic chamber. While the total cost of this system was reported to be approximately 23,000 \$, the bulk of this cost came from the anaerobic chamber (18,000 \$) itself.

While the previous studies reported above provide convincing avenues for researchers to pursue, there are several limitations that need to be addressed. For instance, despite the use of XYθ manipulators, the main usefulness of this type of stage, namely, the formation of twisted 2D heterostructures, has not yet been demonstrated. Second, a low-cost setup can benefit greatly from a light-weight PID-controlled power supply, instead of conventional laboratory power sources, to drive the heating stage. This helps with lowering cost, increases portability, and allows for

quick and easy implementation of the hot pickup process. Third, the versatility of the system to cover other transfer techniques, such as the recently popular capillary-force-assisted wetting polydimethylsiloxane (PDMS) technique,^{15–17} has not been adequately studied. Finally, although the possibility of incorporating such low-cost setups into commercial glovebox systems has been explored,¹⁴ these units are way too expensive for implementation in budget-restricted research groups. This proves an impediment for researchers eager to work with air-sensitive 2D materials.

In this work, we aim to address the abovementioned shortcomings. To this end, we have built an in-house, low-cost transfer system using relatively inexpensive components that are readily available for purchase from online stores. Our system is not only budget-friendly but also compact, lightweight, and customizable and is fully equipped with provisions for PID-controlled substrate heating, thermal isolation for the sample stage, XYZθ and XYZ manipulators, and sample vacuum. We also demonstrate how our portable transfer setup can very easily be installed with a do it yourself (DIY), extremely low-cost (~170 \$), humidity (<4%)- and oxygen (<0.1%)-controlled inert-atmosphere glovebox, allowing for a quick modification/upgrade when an isolated and controlled environment is required for the exfoliation and transfer of more sensitive 2D materials. The low-cost setup is then put to test by evaluating the transfer of 2D materials using several approaches: the hot pickup (dry PDMS-polypropylene carbonate (PPC) stamp) technique,^{10,18–21} the wetting PDMS technique,^{15–17} and a combination of both. We will demonstrate how the combination approach may be ideal to stack specific 2D material candidates. The versatility in the performance of our system is demonstrated with successful creation of hBN-encapsulated graphene (or molybdenum disulphide (MoS₂)) employing the dry transfer technique, MoS₂-hBN, twisted MoS₂, and twisted MoS₂ on hBN using the wetting PDMS technique, and finally, a MoS₂-hBN-graphene structure employing a combination of both dry and

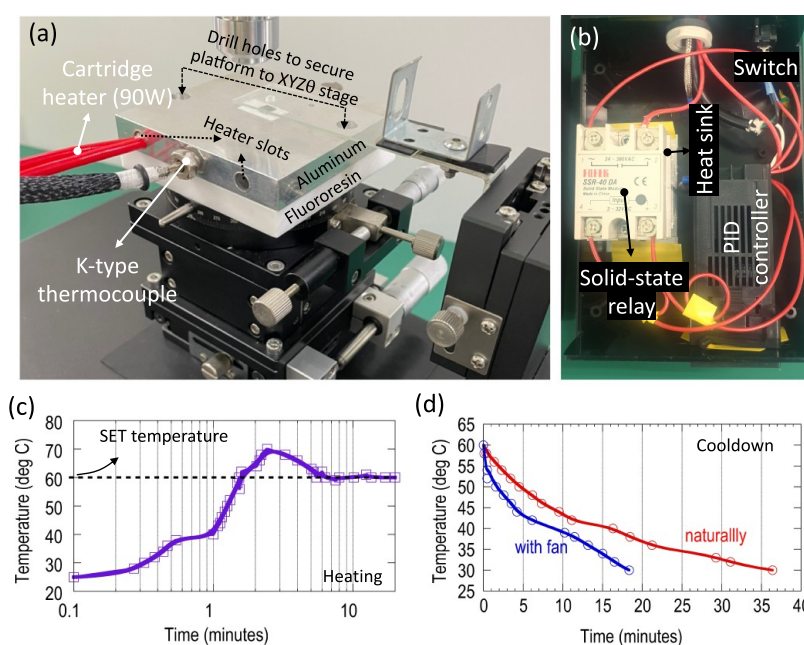


Figure 2. (a) Picture showing the details of construction of the substrate heater assembly. (b) Picture showing the various components used to create the light-weight PID controller unit. (c) Typical PID response for a temperature set at 60 °C, a steady-state condition is reached in about 5 min. (d) Cooldown rate obtained naturally (normal room air) versus that obtained when using a small table fan. “All photographs courtesy of “Ratchanak Somphonsane”. Copyright 2021.”

wet methods. The effectiveness of the DIY glovebox is proven through demonstration of extended stability of freshly exfoliated BP flakes, their encapsulation between thin hBN layers, and the formation of source- and drain-contacted BP devices with a protective hBN top layer.

2. MATERIALS AND DESIGN

2.1. Consumables and Parts. The 2D materials used in this work are graphene, hBN, and BP, obtained via the scotch tape exfoliation method and monolayer MoS₂ domains grown using a single-zone chemical vapor deposition (CVD) tube furnace available in our laboratory. The bulk hBN crystals were provided to our group by NIMS Japan.²² The source materials required for the exfoliation, CVD growth, and the PDMS/PPC stamp creation along with the supplier details and costs are all listed in Table 1.

Table 1 also contains a comprehensive list of all the parts needed to build our base system which comprises the main imaging unit, stages, details of the heating platform, parts for vibration reduction, and finally, the DIY glovebox system that we propose in this work. The overall cost of this system is approximately 1000 \$ which makes this setup a very affordable one. We also propose three optional upgrades: an optical breadboard, a mid-range metallurgical microscope, and provision for sample vacuum. These upgrades will cost an additional 2500 \$, and as we shall describe in the following sections, we believe that they are mostly unnecessary, will make the system bulky, and can therefore be avoided by starting researchers. It is also worth noting that, while the cost of consumables is generally high (~1200 \$ in our case), it is viewed as a one-time investment because source materials typically last for a relatively long period of time.

2.2. Design and Construction. The design of the transfer setup is based on a few basic principles and requirements:

1. A large working distance microscope with reasonable image quality and zoom capabilities.
2. Precision linear stages for XYZ alignment and θ adjustment for rotational alignment.
3. A heated sample stage driven by light-weight PID controllers.
4. Easy incorporation into a glovebox for working with sensitive materials.
5. Overall ease of operation.

Figure 1 shows various images containing the key components of the 2D material transfer system that was built by taking into consideration the abovementioned points. The details of the individual components and the complete system which includes the glovebox setup (see Figure 3) are presented in the following sections.

2.2.1. Imaging System, Linear Stages, and Portability. The imaging system, shown in Figure 1a, consists of a zoom monocular lens package that contains the primary objective lens (0.63–3.5 \times zoom), coaxial light illumination, C-mount for connecting a camera, pillar post, and a light-weight mounting base. An auxiliary 5 \times objective lens with a C-mount adapter is purchased additionally and installed to the primary lens. The combination allows for adjusting the field of view over a wider range with a minimum field of view of roughly 250 \times 250 μm^2 . The primary lens has a field of view ranging from 1 to 6.5 mm².

Figure 1a also shows the two linear stages used in this work. The XYZ stage (left), which is used to manipulate the position of the stamp, is similar to the one used in ref 13, with the top guide plate of the stage positioned vertically. This allows one to increase the level of the glass slide so that the tall height of the XYZ θ (right) stage can be compensated for. A small drawback of this arrangement is that the glass slide containing the stamp (see Figure 1d) needs to be fixed at a 90° angle with the vertical guide plate. To resolve this, we use a general-purpose L-bracket which may be attached (using M3 screws) to any of the mounting hole

positions available on the vertical guide plate. The glass slide containing the PDMS stamp can then be attached to the L-bracket with the help of a flange. The space between the L-bracket and the flange is filled with a silicone pad to avoid breakage of the glass slide (see Figure 1b). XYZ stages with a horizontal top guide plate may also be used (see ref 12), the advantage being that the glass slide may be attached directly onto the guide plate using a double-sided sticky tape. However, the overall height of such a stage is reduced and one may end up needing additional parts to achieve the desired relative height profiles of the two stages.

In contrast to previous studies in which researchers have used an optical breadboard to serve as the base of the system, we deliberately avoided doing so in order to keep the system lightweight and thus portable in its truest sense. The authors in ref 12 have highlighted the importance of such a feature for educators who intend on conducting public demonstrations. While we have found that the lack of a rigid base induces small vibrations in the pillar post, these are mostly excited by the user itself, for instance, when he/she adjusts the focus knob. However, with a little bit of practice using the system, these vibrations do not seem to pose much of an issue. In fact, all heterostructure devices reported in this work have been achieved using the original light-weight (<1 Kg) base. For building a more perfect, vibration-damped system, the optical breadboard is recommended (available from www.standa.it), being mindful of the fact that while it comes at a very reasonable cost, it also weighs a lot (~9 kg) and could be a problem if portability is desired.

Optical breadboards also allow one to securely fasten the linear stages to the base, which helps in suppressing mutual vibrations.¹³ While this seems like a desirable feature to have, we find that simply placing the linear stages on good-quality vibration damping rubber mats and attaching the underside of the base with the vibration damping feet will suffice. This makes it convenient to manually move out the stages when required, for instance, when the user desires frequent access to the stamp assembly for a quick interchange of the stamp. It also helps when a service of optical parts is needed or when the system needs to be lifted and transported.

2.2.2. Substrate Holder. The substrate holder shown in Figure 2a was custom-designed in order to provide heating and vacuum fixation for the sample. Two long cylindrical cavities (6 mm diameter) are first drilled out from a 12 mm-thick Al plate (80 mm × 80 mm) for housing the cartridge heaters (90 W). Since only a modest temperature (50 and 90 °C) is required to carry out the various stages of the hot pickup process, a single cartridge heater would do the job. Alternately, two smaller heaters (45 W each) can also be used. A third hole is drilled and threaded for housing the thermocouple sensor, as shown in Figure 2a. A thermally insulating fluororesin plate, identical in dimensions to the Al plate, is then placed in between the Al plate and the XYZθ stage. Vertically aligned drill holes are made at two precise locations on the Al and fluororesin plates followed by which insulating M3 screws are used to secure the two plates to the XYZθ stage. The fluororesin plate helps isolate the hot plate from the XYZθ stage below and therefore not only avoids overworking of the heaters and the PID controllers but also protects the XYZθ stage from possible damage.

The electrical connections to the cartridge heater and the thermocouple are provided by a simple and lightweight PID controller kit available online for a very affordable cost (only 15 \$). The PID controller works in tandem with a solid-state relay

that toggles the power output to the heaters. The various components are wired and then neatly packed in an electronic enclosure box (see Figures 1a and 2b). The completed unit has a very small footprint and weighs a mere 300 g, which is much less than the weight of a typical laboratory bench power supply. Figure 2c,d shows the typical heating and cooling response of the PID controller, respectively. As seen here, for a temperature value set at 60 °C, a steady state is achieved in about 5 min. The rate of cooldown back to room temperature is conceivably much slower but can be made twice as fast (if desired) with the help of a small cooling fan (Figure 2d). Although not tested in this work, it is expected that even faster cooling should be possible with fitted options such as water (or air) cooling tubes or by the use of a simple heat sink material placed on the top of the hotplate.

For the vacuum attachment, another cylindrical cavity (5 mm diameter) is drilled out at the opposite end to where the cartridge heaters are installed. This horizontal cavity is then made to meet with a tiny hole (2 mm diameter) drilled vertically downward from the center of the Al plate. The primary end of the cavity is threaded and attached with a miniature tube fitting, as shown in Figure 1b, for final connection to a vacuum pump.

While we have shown how a vacuum chuck can be easily made, the requirement of vacuum lines and a pump only adds to system complexity and bulkiness. In addition, the operation of a pump would also likely induce undesirable vibrations. We have considered these issues and therefore decided to instead use a high-temperature, double-side thermal tape commonly used as a heat sink for PCB components. This simple solution works extremely well for hot-plate temperatures up to 120 °C without causing melting of the tape and/or subsequent contamination of the underside of the substrate.

2.2.3. DIY Inert Atmosphere Glovebox. Although commonly used 2D materials such as graphene, hBN, MoS₂, and other transition metal dichalcogenides are stable under atmospheric conditions, certain 2D materials such as BP are very unstable and show signs of oxidative degradation. To work with these materials, it has become necessary to carry out the transfer process in a controlled atmosphere, typical of those provided by anaerobic glovebox systems. Unfortunately, commercial systems such as the one used in ref 14 cost a lot of money and are therefore not an option for many. These systems use chamber evacuation, advanced purge controls, and oxygen scrubbers to lower the O₂ level to few tens (or hundreds) of ppm. On the other hand, there are also mid-price range inert gas gloveboxes that work on the basic principles of air removal and refill via the mechanics of displacement and dilution. While a continuous flow of inert gas is required (no automatic purge controllers), these systems claim to reduce O₂ levels down to less than 10,000 ppm (or 1%), by purging out the oxygen-rich and humid atmospheric air out of the chamber. More information on these gloveboxes can be found at www.cleatech.com. Unfortunately, these gloveboxes are made from acrylic and are therefore very heavy. Moreover, they do not have access windows large enough for convenient insertion and removal of an entire 2D material transfer system. Better strategies are therefore needed.

Here, we present a facile approach of converting a general-purpose storage container (from IKEA) into an inert atmosphere glovebox. Rather than having complicated access ports or load-lock chambers, the container can simply be installed over the transfer setup in a single step and subsequently operated by the user. The light weight of the container and the ease with which the operating environment can be switched as required by the user improves the overall functionality of the

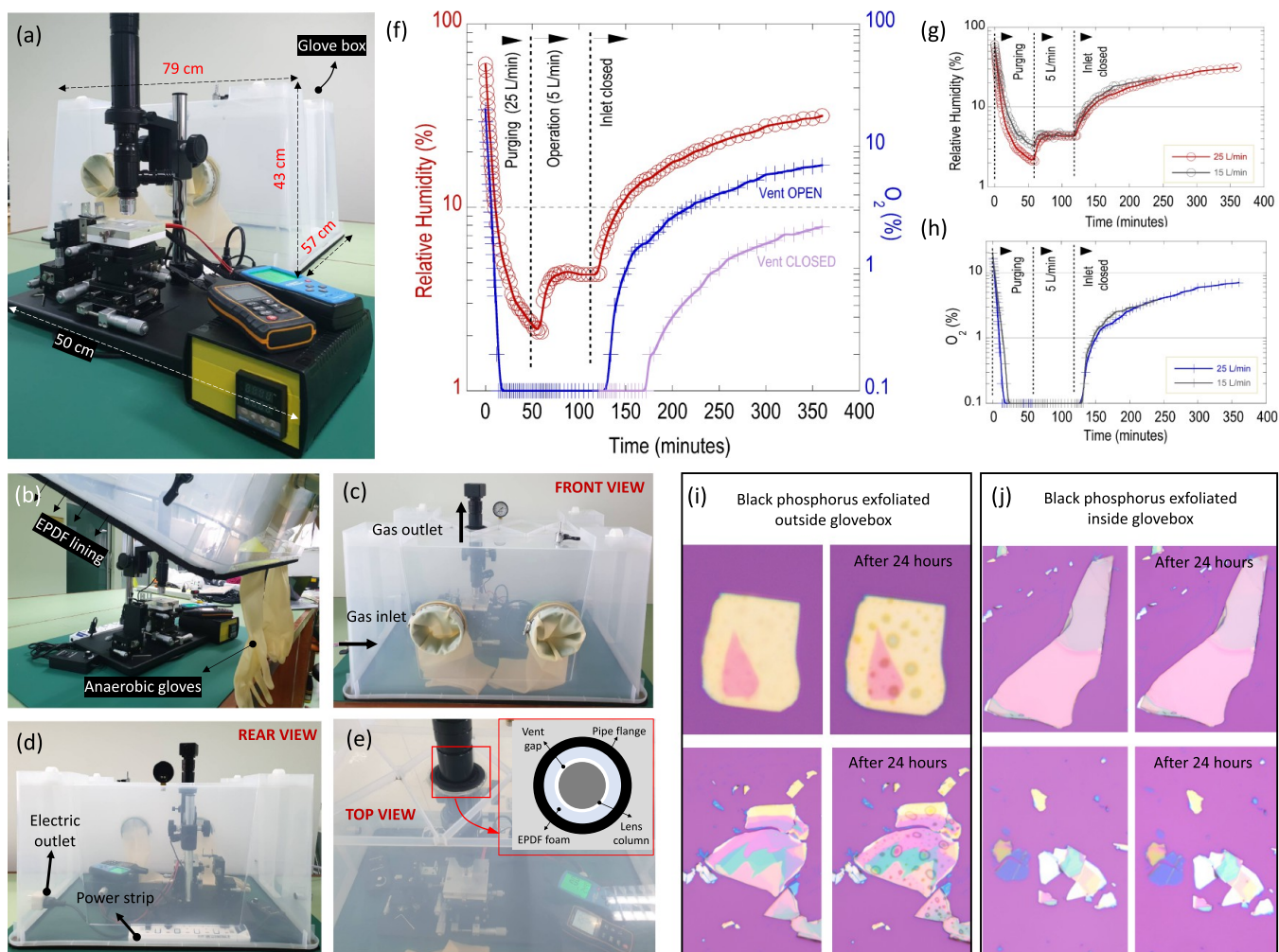


Figure 3. (a) Picture showing the size of the DIY glovebox in relation to the 2D material transfer system. (b) Picture captured during placement of the glovebox over the transfer system. (c) Front and (d) rear views of the glovebox-incorporated transfer system. (e) Top view obtained while the glovebox is under operation. The inset shows a schematic of the vent port (for the gas outlet) arrangement. (f) Data showing the rate of drop in RH and O_2 levels under different nitrogen gas flow conditions of purging and operation of the glovebox. (g) RH and (h) O_2 drop shown for initial purging rates of 25 and 15 L/min. (i) BP flakes exfoliated outside the glovebox (left) with visible damage seen after 24 h (right). (j) BP flakes exfoliated inside the glovebox (left) with no visible damage seen after 24 h (right). “All photographs courtesy of “Ratchanok Somphonsane”. Copyright 2021.”

transfer system by several fold. Basic versions of such a glovebox have been built by DIY enthusiasts for various other purposes. Rather than presenting a detailed construction of the glovebox here, the discussions that follow will be focused on the specific modifications necessary to make the glovebox operate in a highly efficient manner for the specific purpose of working with 2D materials. For building the base version of the glovebox, the reader is encouraged to view videos available online. A few such YouTube links are provided here: [video 1](#), [video 2](#), and [video 3](#).

Figure 3a shows a picture of the customized glovebox used for this work. It can be seen that the dimensions of the box are large enough to comfortably house the transfer system. A few important modifications from the base version were made in order to achieve the best possible performance. First, a high quality, weather-resistant sealing gasket (made from ethylene-propylene diene rubber (EPDM) foam) is used as the lining material around the rim of the box (can be seen in **Figure 3b**). The foam provides the necessary isolation needed to prevent ambient air from seeping into the glove compartment while it is being operated. Second, a large enough hole is drilled on the top of the box to allow for the microscope lens column to pass

through. EPDM foam is then lined along the circumference of the hole, leaving just a small gap to exist between the foam and lens column (**Figure 3e**). This opening is not sealed tight as it will serve as the only outlet port for the inert gas. Alternatively, a taller box (not available to us) that encloses the entire lens column (and camera) could be used. In this case, the power connections to the camera can be fed through the box using a USB feedthrough adapter and the outlet for the gas will be provided by a ball valve, similar to the one used for the input line. Finally, a standard electric outlet is affixed within the box (**Figure 3d**). This outlet connects to a single power strip (also contained within the box) that provides power to the PID controller, microscope light source, and auxiliary camera. This arrangement allows for easy disconnection of the main power line when the glovebox needs to be removed. In addition to the above-mentioned standard modifications, other optional ones can also be entertained. For instance, if the box is semitransparent and a clearer inside view is needed, a view port (made of glass or clear acrylic) can be affixed with epoxy glue after cutting out a required hole from the box.

The glovebox can now be installed following a few easy steps: detach the camera, place the box over the transfer system (Figure 3b), reconnect the camera, connect the inlet gas line, and finally, connect the power cord. Figure 3c–e shows the front, rear, and top views of the transfer system after it has been installed with the glovebox. The inlet gas port is then opened, and either N₂ or Ar gas is allowed inside the chamber. As positive pressure builds inside the box, the ambient air is purged through the outlet port. The RH and the O₂ levels are monitored using the corresponding sensors listed in Table 1. Once an acceptable level is achieved, the user begins the transfer process. It is worthy to note that a perfect hermetic sealing of the glovebox is not a stringent requirement, as the positive pressure ensures that any microscopic leaks are mostly caused by inert gas leaking out of the box and not of the outside air entering in. By taking advantage of this fact, the glovebox reported here has not been designed with a loadlock feature. We found that lifting/tilting one end of the glovebox by just a few centimeters would allow easy exchange of samples and accessories across the glovebox. As long as this action is momentary, it does not affect the RH and O₂ levels. Alternately, if a more sophisticated approach is preferred, a cheap homemade loadlock based on a 10 cm long piece of tube terminated with KF flanges can also be easily constructed and fitted to the glovebox.

A typical operating sequence, which we have used, starts with purging the chamber with a high gas flow rate of ~25 L/min for about 1 h. This is followed by lowering the flow rate to ~5 L/min and subsequently maintaining it at this level for an additional 1 h. During this time, the user performs his/her transfer task. Upon completion, the gas inlet is shut off and the operator removes the sample. Figure 3f shows the results obtained for the drop in O₂ and humidity levels as a function of time and with respect to the corresponding N₂ gas flow conditions. It can be seen that our system is capable of reducing the RH levels within the working area from 63% to less than 5% in just under 10–15 min of N₂ gas purging. During this time, the O₂ level has already dropped from 21% to less than 0.1% (or 1000 ppm). At the end of the purging interval, the RH value drops to the lowest point of roughly 2.1%. Once the purging is complete and the flow rate is lowered to 5 L/min, the RH value is seen to initially increase but quickly settles at a steady-state value of ~4%. Remarkably, these metrics are achieved without the need for chamber evacuation, purge control, or expensive oxygen scrubbers.

In contrast to the results presented in Figure 3f, a commercial anaerobic chamber (see ref 14, for instance) takes about 6 h to achieve a 0.1% O₂ level (~3 h with the oxygen scrubber turned on). The longer time is possibly due to the large chamber volume that needs to be evacuated and purged. Moreover, if frequent access to the glovebox is needed, this means the system needs to be powered on and operated continuously throughout the working day, which is evidently resource-consuming. The remarkable sealing performance of the DIY glovebox presented here is further illustrated in Figure 3f, where the rate of RH (and O₂) increase post shutting off the inert gas supply is seen to be at least a few orders of magnitude slower than the rate of the initial decrease. Importantly, this is the case when the vent valve is left open. As seen in Figure 3f, if the vent is fully closed, then the inert conditions within the box can be maintained for a much longer time. Ideally, a taller box fully enclosing the transfer system will allow for this kind of operation and will consequently also help reduce the usage of N₂ gas. In our current mode of operation, a standard cylinder of high-purity compressed N₂ would last for up to three full operation cycles if an initial purge

rate of 15 L/min is used. This translates to a running cost of roughly 5–10 \$ per time of use, depending on the location. For further reduction in gas consumption, chamber evacuation prior to purging will be needed, and this is definitely possible if one has access to a suitable glovebox made from acrylic or glass.

To further substantiate the prolonged maintenance of inert conditions within the glovebox, we have tested the stability of freshly exfoliated BP flakes. As shown in Figure 3i,j, for BP flakes exfoliated under ambient conditions, severe damage (in the form of acid bubbles) is observed after 24 h of exposure to air. On the other hand, when the exfoliation is performed within the glovebox and the sample is left inside post operation, there is no visible damage observed on the BP flakes when viewed 24 h later under a high-resolution microscope. It is important to note that the BP sample is well protected inside the glovebox even though the inlet gas flow has been fully shut off, proving once again the effectiveness of the glovebox's sealing performance, much of which is believed to be due to the superior qualities of the EPDM foam lining.

Figure 3g,h shows the effect of the gas purging rate on the lowering of the RH and O₂ values, respectively. With a slower purge rate of 15 L/min, the RH drops to about 3.5% in 1 h. Interestingly, once the rate is lowered to 5 L/min, the RH value is seen to once again settle at a steady-state value of ~4%. This seems to indicate a maximum performance limit being reached for the given conditions of the glovebox. The most likely contributing factors for this are the imperfect seals and nonhermetic feedthrough connections. Conceivably, both of these factors can be further optimized to improve the ultimate performance of the glovebox.

Quite astonishingly, the superior performance metrics of the glovebox discussed thus far is attainable at a mere price total of ~170 \$, with the bulk of the expense taken by the humidity and O₂ meters (~110 \$) alone. In comparison, a commercially available anaerobic glovebox may cost upward of 15,000 \$. Table 2 provides a specification list for the low-cost transfer setup along with the DIY glovebox used in this work. Overall, we believe that the DIY option presented here is a high-performance, user-friendly, and an extremely low-cost alternative that can be exploited by any lay person, student, or researcher who is interested in exploring the fascinating aspects of 2D materials.

3. RESULTS AND DISCUSSIONS

We now demonstrate how versatile our transfer setup can be in creating both simple and complicated heterostructures. To this end, we employ the popular hot pickup (dry transfer) technique,¹⁸ a recently reported wetting PDMS technique¹⁷ (no heat), and a combination of both these techniques, to create the various heterostructures listed in Table 3. The general difficulty levels, judged from the number of successfully formed heterostructures, can also be seen here. It is also important to note that the wetting transfer could not be carried out in a very low humidity environment, and therefore, the glovebox use is limited to only the dry transfer method.

3.1. Dry PDMS-PPC (Hot Pickup). The widely popular hot pickup technique has been used by various research groups due to its effectiveness in creating heterostructure stacks. A typical process flow starts with the creation of a transparent PDMS film cut into a small square (2 mm by 2 mm) to form a stamp-like structure. A thin layer of PPC is then spun on top to create a PDMS-PPC stack followed by affixing it to a glass slide (see Figure 1d).

Table 2. Specifications of the Transfer Setup

| item | specification/provision |
|--------------------------|--|
| imaging system | zoom microscope objective: 0.63–3.5 \times (about 62–1000 \times on the display) mount: C-mount for PC or TV camera connection working distance: 9.3–10 mm field of view: 1–6.5 mm illumination: coaxial light light power input: 110–240 V, 50–60 HZ, auto switching pillar: 260 mm long CMOS camera: 5 megapixels |
| linear stages | XY axis \pm 12.5 mm, Z axis 10 mm, 0.01 mm resolution R-axis 360 $^\circ$ coarse, 5 $^\circ$ fine, 0.16 $^\circ$ resolution |
| substrate heating system | heating stage (12 mm Al plate, safe temperature range 25–200 $^\circ$ C) 10 mm-thick fluororesin plates for thermal isolation from linear stages lightweight PID control unit (25–1300 $^\circ$ C) substrate vacuum provision |
| DIY Glovebox | relative humidity: 63% RH to <5% RH under 15 min with N ₂ purging at 25 L/min 4% RH steady state at 5 L/min oxygen level: rapid lowering: 22% to less than 0.1% under 10 min gradual rise: 0.1–2% in 3 h with vent valve closed high quality EPDM foam lining anaerobic gloves standard 230 V adapter 1/8" ball valves for gas inlet and outlet other features tailorable as per requirements |
| meters/sensors | RH meter: 0–100% range, 0.1% resolution oxygen meter: resolution 0.1% (1000 ppm), minimum reading 0.0% (recommend upgrade to a trace oxygen meter for <1000 ppm detection) |

Figure 4a shows a schematic of various stages involved in the creation of an hBN-encapsulated graphene heterostructure. First, a potential hBN flake is picked up from the substrate by lowering the stamp onto the substrate, making contact with the hBN, and then lifting it up. All the while, the substrate is maintained at a temperature near 40 $^\circ$ C to facilitate the pickup of the underlying hBN. The stamp carrying the hBN is then brought into contact with a graphene flake. As the stamp is

retrieved, the graphene flake attaches itself to the hBN forming a graphene-hBN-PPC stack. This stack is once again lowered onto a different hBN flake located on a substrate kept at 90 $^\circ$ C. Upon retrieval of the stamp, the fully formed encapsulated graphene stack is left behind.

Figure 4b shows the optical images captured by the low-cost transfer setup at various stages of the creation of an hBN-encapsulated graphene heterostructure while operating within the glovebox. Optical images of the fully formed heterostructure shown in panels (v,vi) of Figure 4b are those obtained by the low-cost setup and a high-resolution microscope, respectively. Although the operation within the glovebox causes some difficulty for the user in obtaining very crisp images, the ones shown in Figure 4b [see also (e,f)] are nonetheless of sufficient quality needed for a successful transfer. If working outside the glovebox, the user may alternatively choose to obtain better quality images using a secondary high-resolution microscope (if available). The inset of Figure 4c shows such an image obtained after graphene flakes were picked up by hBN. The inset of Figure 4d shows a similar image for MoS₂ picked up by hBN. It is also important to note that the images captured in Figure 4a are the images as seen by the user without unmounting the glass slide at any stage of the transfer process. While the image quality is ultimately limited by the depth of focus and resolution of the microscope, the process can become slightly more challenging since the picked up hBN flake needs to be focused through the glass slide and a thick layer of PDMS stamp. The focusing is particularly difficult to achieve if the hBN flakes are too thin. We therefore find it important that the PDMS stamp and the glass slide should be clear and no intermediate adhesive layers should be used.

In order to prove that the glovebox is truly functional, we have used it to successfully assemble heterostructures based on BP. The various panels shown in Figure 4e capture the steps involved in the encapsulation of a thin BP flake. After assembly, the sample is removed from the glovebox to obtain a detailed optical image [see panel (iv) of Figure 4e which reveals the successful encapsulation of the BP flake between two thin layers of hBN]. To further demonstrate the versatility of our setup, we have also assembled source- and drain-contacted BP devices with a protective hBN layer on top. The top and bottom panels of Figure 4f capture the steps involved in creating two such devices. In this work, we have used prefabricated Pt contacts on

Table 3. List of all Device Architectures Created Using the Low-Cost Setup

| stamp method | heterostructures | number of successful samples/total attempts | difficulty |
|-----------------------------|---|---|------------|
| dry PDMS-PPC (hot pickup) | non hBN-assisted | | |
| | (1) Graphene-hBN | 1/6 | hard |
| | (2) MoS ₂ -hBN | 0/8 | hard |
| | hBN-assisted | | |
| | (1) hBN-BP-hBN (glovebox) | 4/6 | easy |
| | (2) hBN-BP-contacts (glovebox) | 3/5 | medium |
| wetting PDMS (no heat) | (3) hBN-graphene-hBN ^a | 5/7 | easy |
| | (4) hBN-MoS ₂ -hBN | 2/4 | medium |
| | (1) Graphene-hBN | 3/7 | medium |
| | (2) MoS ₂ -hBN | 2/2 | easy |
| combination (dry + wetting) | (3) twisted MoS ₂ on Si/SiO ₂ | 8/10 | easy |
| | (4) twisted MoS ₂ on hBN | 1/1 | easy |
| | (1) MoS ₂ -hBN-graphene | 1/3 | easy |

^aFew candidates made inside the glovebox.

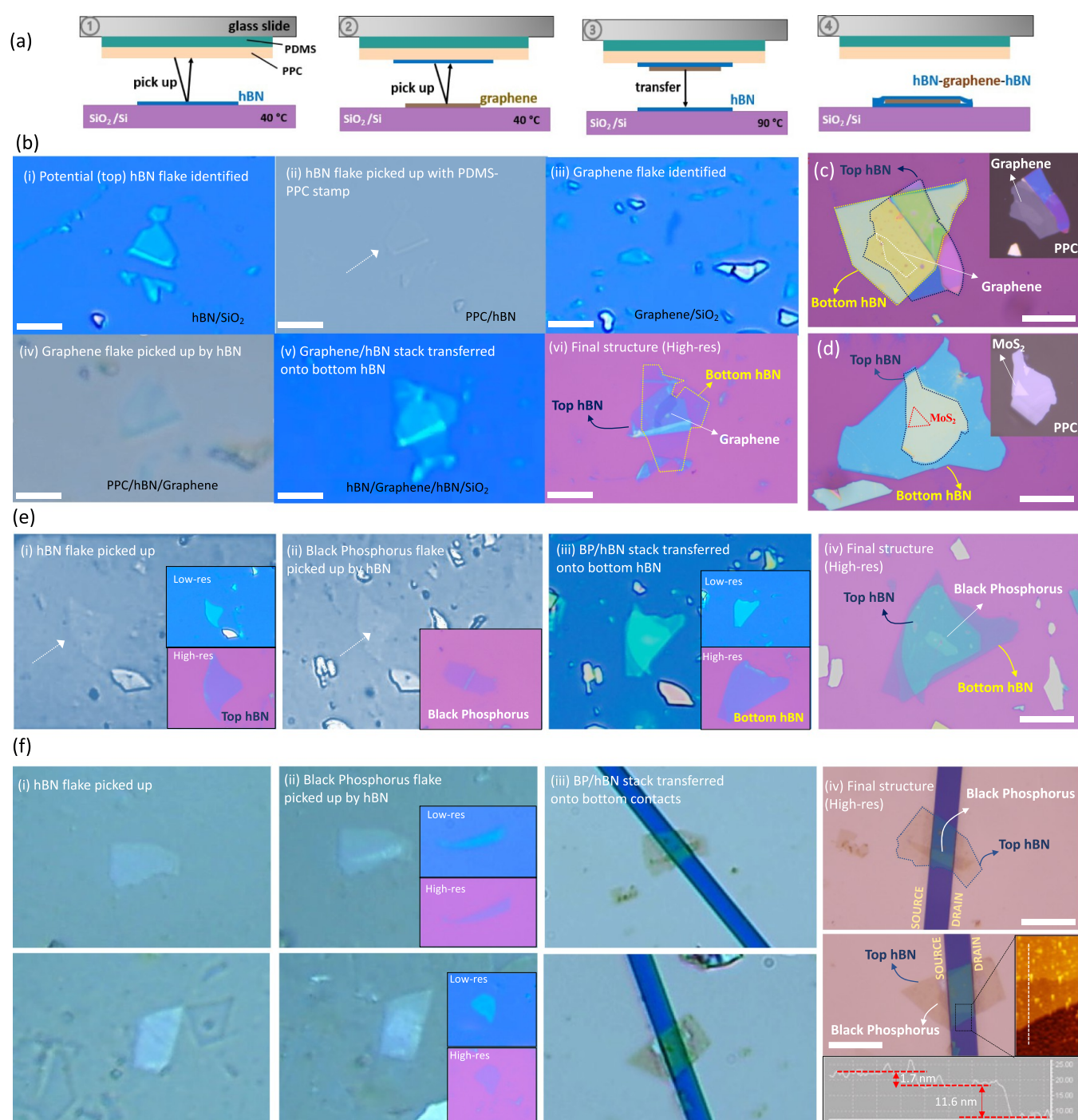


Figure 4. (a) Schematic showing the various steps involved in the hot pickup process. (b) Optical images as viewed with the low-cost transfer setup (and operated within the glovebox) obtained at various stages (i–v) of the creation of an hBN-encapsulated graphene heterostructure. Optical image obtained of the final structure from a high-resolution microscope is seen in (vi). (c) Optical image taken with a high-resolution microscope capturing the fully formed heterostructure of another hBN-encapsulated graphene device made outside the glovebox. The inset shows the high-resolution image obtained after the pickup of graphene by hBN. (d) Images similar to (c) but for an hBN-encapsulated MoS₂ device. (e) Optical images capturing the various stages of creating an hBN-encapsulated BP heterostructure and (f) optical images capturing various stages of assembly of source- and drain-contacted BP devices [device 1 (top) and device 2 (bottom)] topped with a protective hBN layer. The inset to panel (iv) of device 2 shows the AFM scan and thickness measurement of the final assembled device. All scale bars are 20 μm .

Si/SiO₂ wafers (purchased from Ossila) to serve as the bottom source and drain contacts. To complete the remaining assembly, an hBN flake, which eventually serves as the top protective layer, is used to pick up the BP flake, followed by carefully aligning and placing the combination between the source and drain contacts.

As an additional note, while our low-cost imaging system does fairly well in identifying potential graphene and MoS₂ flakes, we found it slightly more difficult to gauge the thickness of BP flakes to be able to select thin ones. Occasionally, therefore, post exfoliation inside the glovebox, the samples would be taken out of the glove box (for a very short while) to optically judge the

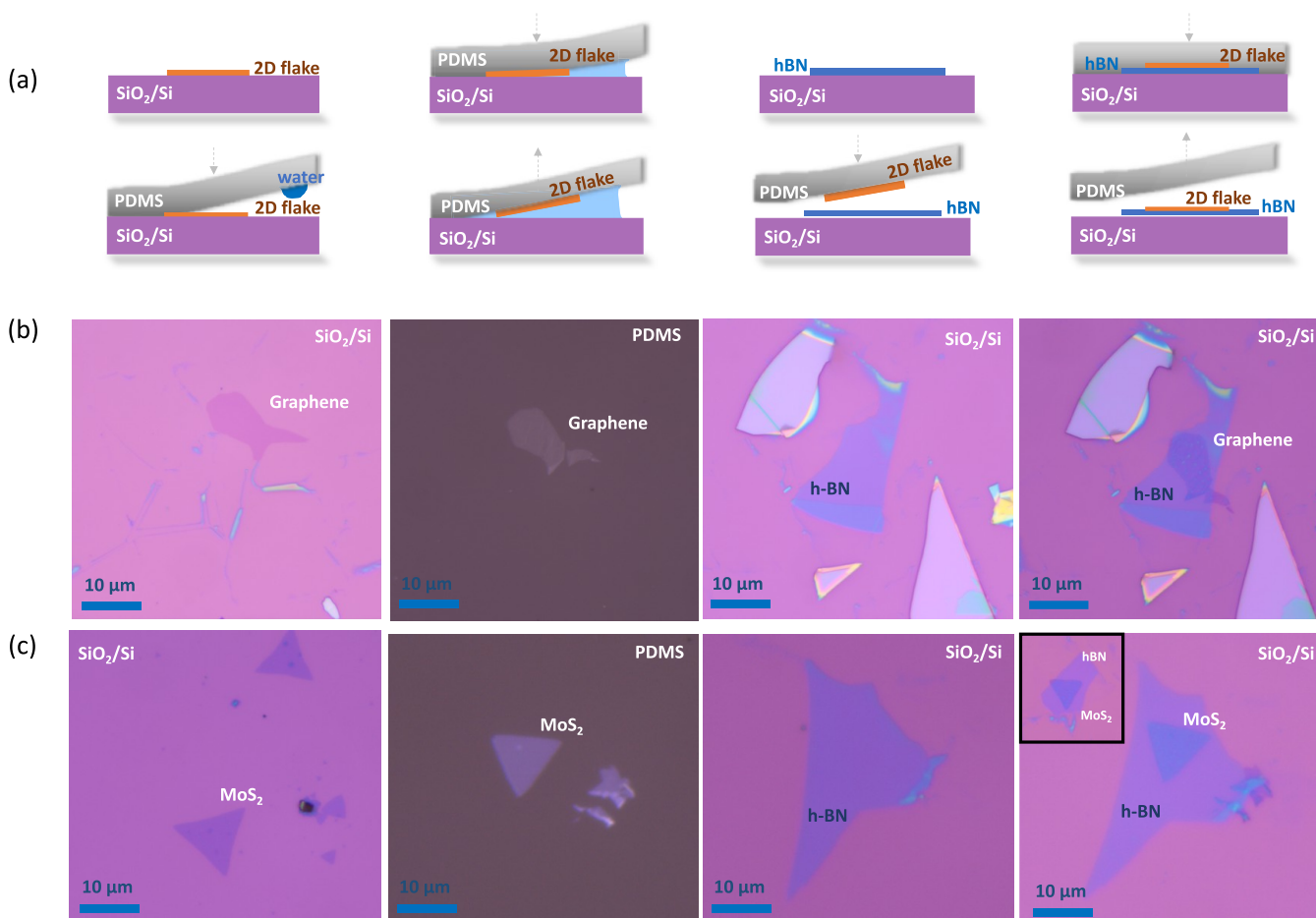


Figure 5. (a) Schematic showing the various steps involved in the wetting PDMS method. High-resolution optical images capturing the formation of a (b) graphene-hBN and (c) MoS₂-hBN structure following the steps shown in (a). The inset to the right most panel of (c) shows a picture of a second device obtained using the same method.

thickness of the preselected BP flakes using the high-resolution microscope but also ensuring that they were quickly returned to the glovebox to carry out the subsequent heterostructure assembly. The insets of panel (ii) in Figure 4f show a comparison of the low and high-resolution images of the identified thin BP flake. AFM scans obtained post the final assembly of the device shown in the bottom panel of Figure 4f revealed a BP thickness of 1.7 nm and the top BN thickness of approximately 11.5 nm. Although the act of moving the sample in and out of the glovebox for flake verification is not ideal, it is only a small inconvenience. Having said that, an upgrade to a good metallurgical microscope should be seriously considered, especially for critical device assemblies where removal of the sample from the glovebox for even a short period of time, post exfoliation, cannot be afforded.

Although the hot pickup method described above worked well for forming encapsulated structures with both graphene and BP, we found that the success rate for hBN-encapsulated MoS₂ formation was significantly lower. In many instances, after making contact with the flake and subsequent retrieval of stamp, the MoS₂ flake is partially lifted and/or severely damaged. The reason for such damage is unclear, although this may be an indication that the high-temperature (~ 750 °C) CVD process could have caused the flake to adhere to the substrate much more strongly in comparison to an exfoliated sample. Moreover, varying pickup parameters, such as the substrate temperature, did not result in a better outcome. In addition to this, it is also

well known that picking up a graphene or MoS₂ using direct contact with the PDMS-PPC stamp is not only difficult but the process is also not clean due to polymer contamination. The apparent ineffectiveness to employ a direct pickup sequence (i.e., without the assistance of hBN) for creation of “non-hBN-sandwiched” heterostructures such as MoS₂ on hBN or twisted MoS₂ on Si/SiO₂ (or hBN) renders the hot pickup process rather limiting in its capabilities.

3.2. Wetting PDMS. Recently, a wetting PDMS method based on a capillary-force-assisted stamp technique was reported.^{10–12} This technique differs from the dry stamp method in that the function of the PPC layer, which is to enhance the adhesion of the 2D material to the stamp, is replaced with a thin evaporative liquid such as water. As the liquid finds its way between the interface of the PDMS surface and the 2D material, the capillary forces cause the 2D material to be lifted up from the substrate. This method has been shown to be effective in not only transferring 2D materials from one substrate to another but also, more recently, forming twisted graphene structures¹⁷ without causing mechanical damage.

As shown in Figure 5a, the wetting process generally starts by placing a tiny drop of water on the underside of the PDMS stamp. The stamp is then very gradually lowered onto the flake of interest. Upon initial contact, the edge of the water front becomes visible in the microscope. The user then very carefully lowers the stamp so as to maintain a slow movement of the water front as it moves across the flake. After this, the PDMS stamp is

raised and the lifted flake can be seen to adhere to the PDMS layer, indicating a successful liftoff. At this stage, the water film has already evaporated and the flake can be transferred onto another substrate for either relocation or stacking with another flake.

The authors of ref 17 have discussed the importance of using a wedge-shaped PDMS stamp and the need for a hydrophilic substrate for obtaining good results. While our samples have been plasma-treated prior to exfoliation and undergoing transfer, a standard rectangular PDMS (instead of wedge PDMS) was able to give a decent outcome for forming simple structures such as graphene on hBN (see Figure 5b) and MoS₂ on hBN (see Figure 5c). The effectiveness of our transfer setup in using the wetting method is further demonstrated in Figure 6a–c, where we show examples of twisted MoS₂ domains

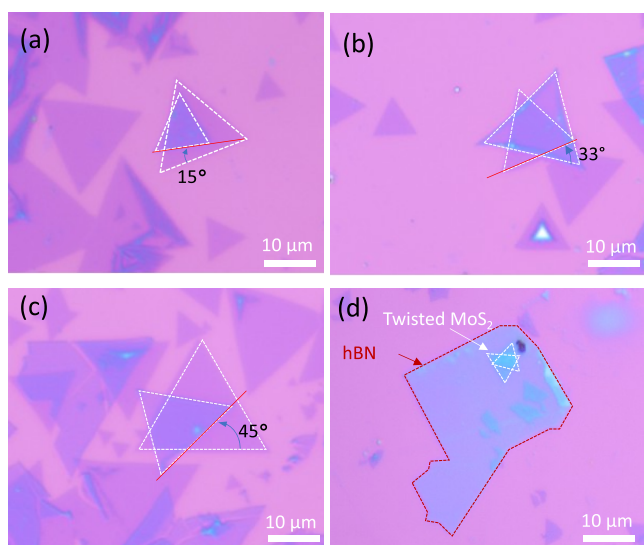


Figure 6. (a) Twisted MoS₂ heterostructures with different twist angles of (a) 15°, (b) 33°, and (c) 45° formed on Si/SiO₂ using the wetting PDMS technique. (d) Twisted MoS₂ formed on a thin layer of hBN.

transferred on the Si/SiO₂ substrate with several different twist angles (15, 33, and 45°) made between the top and bottom MoS₂ layers. Additionally, Figure 6d shows an example of a twisted MoS₂ bilayer transferred onto a thin layer of hBN.

A challenging aspect of the wetting transfer process is the difficulty in controlling the speed of the moving water front across the interface due to this process being a manually operated one. We therefore anticipate that for a more comprehensive evaluation of the wetting technique, the use of a motorized stage, to achieve precise control, may be beneficial.

3.3. Combination Approach. From the preceding discussions, the importance of using a combination of dry and wet methods might already be evident. 2D materials that adhere strongly to the substrate may not be easily transferred using the hot pickup method and can therefore be approached with the wetting PDMS method instead. At the same time, the widely established hot pickup method may be employed to reliably pick up mechanically exfoliated flakes such as hBN. A combination of both techniques applied in a sequential manner may then be visualized for creating various possible combinations. In this work, we have used this approach to create a graphene-hBN-MoS₂ vertical tunneling-type structure. The hBN flake (obtained via exfoliation) is first picked up using the hot pickup method and placed on top of a graphene flake. This is then followed using the wetting transfer to place a potential MoS₂ flake on top of the graphene-hBN stack. Figure 7 shows the images obtained at various stages of the transfer process.

4. CONCLUSIONS

In conclusion, we have demonstrated a versatile and low-cost 2D material transfer setup that can be constructed with ease in any minimally equipped laboratory setting, budget-restricted or otherwise. In comparison to other recent setups reported in the literature, our system is compact, lightweight, and portable and is custom-built for more functionalities such as substrate heating using PID controllers and vacuum fixation of the sample. Due to its overall light weight, the transfer system reported here can be easily lifted and transported by a single individual, a convenience sought by educators wanting to perform public demonstrations related to 2D material physics.

The versatility of our transfer system has been tested by employing three different transfer techniques. These include the popular hot pickup (dry PDMS) method, a recently reported wetting PDMS method, and a combination method not reported previously. We have found that while the hot pickup method works well for exfoliated samples, they do not perform well with CVD-grown MoS₂ flakes. In contrast, the wetting

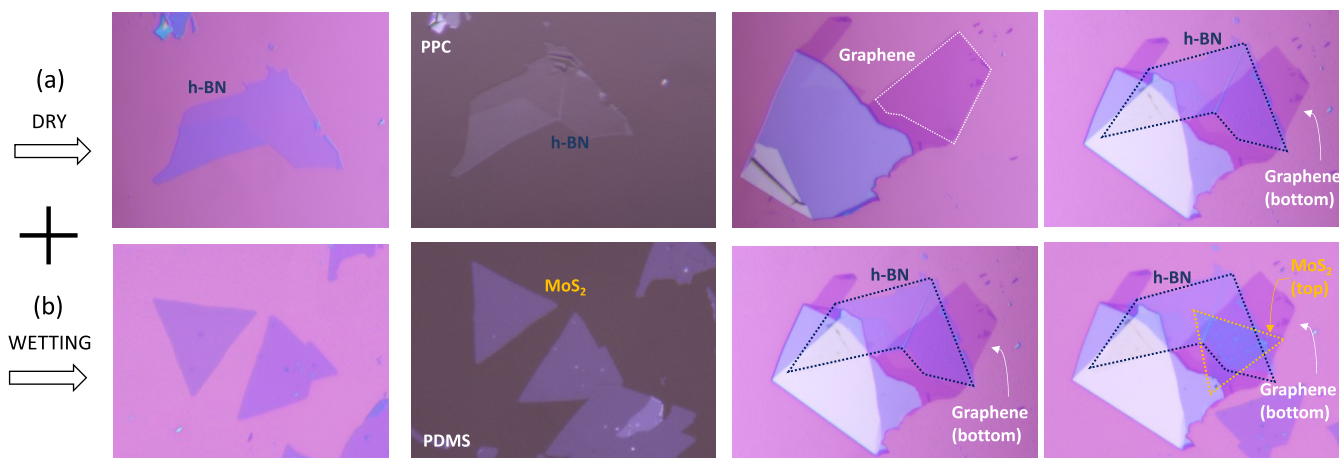


Figure 7. Optical images capturing various stages of a MoS₂-hBN-graphene heterostructure formation using a combination of (a) dry and (b) wetting sequences.

method creates the transfer-favorable conditions needed to overcome the apparently high adhesion energy of the CVD flake to the substrate. Using this approach, we have successfully demonstrated the creation of twisted MoS₂ heterostructures obtained on Si/SiO₂ (or hBN) with varying twist angles. Using the combination method, we have demonstrated the creation of a vertical tunneling structure of MoS₂-hBN-graphene.

A significant highlight of our work is the design and construction of a low-cost, DIY inert atmosphere glovebox. The performance of the glovebox as it relates to its ability to reduce humidity and O₂ levels is found to be at par with commercially available anaerobic glovebox systems. Most importantly, the glovebox can be rapidly incorporated with the transfer system when working with ambient-sensitive 2D materials is required. In this work, we have demonstrated the effectiveness of such a combination with the successful encapsulation of BP inside the glovebox and the assembling of source- and drain-contacted BP devices.

The “all-in-one” 2D material transfer system reported here is the first of its kind and is expected to contribute toward the overall growth of 2D material research by making available a cost-effective, user-friendly, and high-performance alternative to scientific communities spread across the world.

AUTHOR INFORMATION

Corresponding Author

Harihara Ramamoorthy – Department of Electronics Engineering, Faculty of Engineering, King Mongkut's Institute of Technology Ladkrabang, Bangkok 10520, Thailand; orcid.org/0000-0002-4282-2948; Email: harihara.ra@kmitl.ac.th

Authors

Kanokwan Buapan – Department of Physics, Faculty of Science, King Mongkut's Institute of Technology Ladkrabang, Bangkok 10520, Thailand

Ratchanok Somphonsane – Department of Physics, Faculty of Science, King Mongkut's Institute of Technology Ladkrabang, Bangkok 10520, Thailand; Thailand Center of Excellence in Physics, Commission on Higher Education, Bangkok 10400, Thailand

Tinna Chiawchan – Department of Physics, Faculty of Science, King Mongkut's Institute of Technology Ladkrabang, Bangkok 10520, Thailand

Complete contact information is available at:

<https://pubs.acs.org/10.1021/acsomega.1c01582>

Author Contributions

K.B.—Mechanical exfoliation of graphene, hBN, and BP. Low-cost 2D material transfer system setup and testing. R.S.—Design of experiments, project supervision, and review and editing of the manuscript. T.C.—CVD growth of MoS₂. H.R.—Manuscript writing, figure and data analysis, and glovebox design and testing.

Notes

The authors declare no competing financial interest.

ACKNOWLEDGMENTS

This research has received funding support from the NSRF via the Program Management Unit for Human Resources & Institutional Development, Research and Innovation (grant number B05F630084). H.R. acknowledges support from King

Mongkut's Institute of Technology Ladkrabang (grant no KREF046302). We extend our sincere thanks to Prof. Takashi Taniguchi of NIMS Japan for providing us with high-quality hBN crystals without which this work could not have been successfully carried out. We also thank Asst. Prof. Thiti Taychatanapat of Chulalongkorn University, Bangkok, for valuable discussions.

ABBREVIATIONS

| | |
|------------------|---------------------------------|
| DIY | do it yourself |
| 2D | two-dimensional |
| hBN | hexagonal boron nitride |
| BP | black phosphorus |
| CVD | chemical vapor deposition |
| MoS ₂ | molybdenum disulfide |
| PDMS | polydimethylsiloxane |
| PPC | polypropylene carbonate |
| EPDM | ethylene-propylene diene rubber |
| TMD | transition metal dichalcogenide |
| Pt | platinum |

REFERENCES

- (1) Geim, A. K.; Grigorieva, I. V. Van der Waals heterostructures. *Nature* **2013**, *499*, 419–425.
- (2) Liu, Y.; Weiss, N. O.; Duan, X.; Cheng, H.-C.; Huang, Y.; Duan, X. Van der Waals heterostructures and devices. *Nat. Rev. Mater.* **2016**, *1*, 16042.
- (3) Novoselov, K. S.; Mishchenko, A.; Carvalho, A.; Castro Neto, A. H. 2D materials and van der Waals heterostructures. *Science* **2016**, *353*, aac9439.
- (4) Jariwala, D.; Marks, T. J.; Hersam, M. C. Mixed-dimensional van der Waals heterostructures. *Nat. Mater.* **2017**, *16*, 170–181.
- (5) Frisenda, R.; Navarro-Moratalla, E.; Gant, P.; Pérez De Lara, D.; Jariillo-Herrero, P.; Gorbachev, R. V.; Castellanos-Gomez, A. Recent progress in the assembly of nanodevices and van der Waals heterostructures by deterministic placement of 2D materials. *Chem. Soc. Rev.* **2018**, *47*, 53–68.
- (6) Yankowitz, M.; Ma, Q.; Jariillo-Herrero, P.; LeRoy, B. J. van der Waals heterostructures combining graphene and hexagonal boron nitride. *Nat. Rev. Phys.* **2019**, *1*, 112–125.
- (7) Kim, K.; Yankowitz, M.; Fallahzad, B.; Kang, S.; Movva, H. C. P.; Huang, S.; Larentis, S.; Corbet, C. M.; Taniguchi, T.; Watanabe, K.; Banerjee, S. K.; LeRoy, B. J.; Tutuc, E. van der Waals Heterostructures with High Accuracy Rotational Alignment. *Nano Lett.* **2016**, *16*, 1989–1995.
- (8) Cao, Y.; Fatemi, V.; Fang, S.; Watanabe, K.; Taniguchi, T.; Kaxiras, E.; Jariillo-Herrero, P. Unconventional superconductivity in magic-angle graphene superlattices. *Nature* **2018**, *556*, 43–50.
- (9) Lin, M.-L.; Tan, Q.-H.; Wu, J.-B.; Chen, X.-S.; Wang, J.-H.; Pan, Y.-H.; Zhang, X.; Cong, X.; Zhang, J.; Ji, W.; Hu, P.-A.; Liu, K.-H.; Tan, P.-H. Moiré Phonons in Twisted Bilayer MoS₂. *ACS Nano* **2018**, *12*, 8770–8780.
- (10) Zomer, P. J.; Guimarães, M. H. D.; Brant, J. C.; Tombros, N.; van Wees, B. J. Fast pick up technique for high quality heterostructures of bilayer graphene and hexagonal boron nitride. *Appl. Phys. Lett.* **2014**, *105*, 013101.
- (11) Castellanos-Gomez, A.; Buscema, M.; Molenaar, R.; Singh, V.; Janssen, L.; van der Zant, H. S. J.; Steele, G. A. Deterministic transfer of two-dimensional materials by all-dry viscoelastic stamping. *2D Mater* **2014**, *1*, 011002.
- (12) Zhao, Q.; Wang, T.; Ryu, Y. K.; Frisenda, R.; Castellanos-Gomez, A. An inexpensive system for the deterministic transfer of 2D materials. *J. Phys. Mater.* **2020**, *3*, 016001.
- (13) Martanov, S. G.; Zhurbina, N. K.; Pugachev, M. V.; Duleba, A. I.; Akmaev, M. A.; Belykh, V. V.; Kuntsevich, A. Y. Making van der Waals Heterostructures Assembly Accessible to Everyone. *Nanomaterials* **2020**, *10*, 2305.

(14) Gant, P.; Carrascoso, F.; Zhao, Q.; Ryu, Y. K.; Seitz, M.; Prins, F.; Frisenda, R.; Castellanos-Gomez, A. A system for the deterministic transfer of 2D materials under inert environmental conditions. *2D Mater.* **2020**, *7*, 025034.

(15) Ma, X.; Liu, Q.; Xu, D.; Zhu, Y.; Kim, S.; Cui, Y.; Zhong, L.; Liu, M. Capillary-Force-Assisted Clean-Stamp Transfer of Two-Dimensional Materials. *Nano Lett.* **2017**, *17*, 6961–6967.

(16) Zhang, Y.; Liu, Q.; Xu, B. Liquid-Assisted, Etching-Free, Mechanical Peeling of 2D Materials. *Extreme Mech. Lett.* **2017**, *16*, 33–40.

(17) Hou, Y.; Ren, X.; Fan, J.; Wang, G.; Dai, Z.; Jin, C.; Wang, W.; Zhu, Y.; Zhang, S.; Liu, L.; Zhang, Z. Preparation of Twisted Bilayer Graphene via the Wetting Transfer Method. *ACS Appl. Mater. Interfaces* **2020**, *12*, 40958–40967.

(18) Pizzocchero, F.; Gammelgaard, L.; Jessen, B. S.; Caridad, J. M.; Wang, L.; Hone, J.; Bøggild, P.; Booth, T. J. The hot pick-up technique for batch assembly of van der Waals heterostructures. *Nat. Commun.* **2016**, *7*, 11894.

(19) Wang, L.; Meric, I.; Huang, P. Y.; Gao, Q.; Gao, Y.; Tran, H.; Taniguchi, T.; Watanabe, K.; Campos, L. M.; Muller, D. A.; Guo, J.; Kim, P.; Hone, J.; Shepard, K. L.; Dean, C. R. One-Dimensional Electrical Contact to a Two-Dimensional Material. *Science* **2013**, *342*, 614–617.

(20) Tien, D. H.; Park, J.-Y.; Kim, K. B.; Lee, N.; Choi, T.; Kim, P.; Taniguchi, T.; Watanabe, K.; Seo, Y. Study of Graphene-based 2D-Heterostructure Device Fabricated by All-Dry Transfer Process. *ACS Appl. Mater. Interfaces* **2016**, *8*, 3072–3078.

(21) Iwasaki, T.; Endo, K.; Watanabe, E.; Tsuya, D.; Morita, Y.; Nakaharai, S.; Noguchi, Y.; Wakayama, Y.; Watanabe, K.; Taniguchi, T.; Moriyama, S. Bubble-Free Transfer Technique for High-Quality Graphene/Hexagonal Boron Nitride van der Waals Heterostructures. *ACS Appl. Mater. Interfaces* **2020**, *12*, 8533–8538.

(22) Zastrow, M. Meet the crystal growers who sparked a revolution in graphene electronics. *Nature* **2019**, *572*, 429–432.